

# Novel Resonant Converter Topology Realized by Adjusting Transformer Parameters

Chandan Chakraborty\*, *Member IEEE* Muneaki Ishida\*, *Member IEEE* and Yoichi Hori\*\*, *Member IEEE*

\* Department of Electrical & Electronic Engineering,  
Mie University,  
1515 Kamihama, Tsu, Mie 514-8507, Japan  
Email: chakraborty@ieee.org m.ishida@ieee.org

\*\* Department of Electrical Engineering,  
University of Tokyo,  
7-3-1 Hongo, Bunkyo, Tokyo, 113-8656, Japan  
E-mail: hori@hori.t.u-tokyo.ac.jp

## Abstract

*This paper shows a new direction as to how the transformer parameters may be best utilized and presents the performance and control of novel DC/DC and AC/DC converter topologies. All the three inductances of a transformer have been utilized to realize a  $CL^3$  topology having excellent characteristics and requiring no external inductor. For half bridge topology the capacitor used for the purpose of input voltage splitting also serves as the resonating capacitor. Thus in the half bridge version the topology is realized only with a specially designed transformer and no other external components. A laboratory setup is produced and experiments conducted for DC/DC and AC/DC applications. New design procedure and control technique for the converters also presented. These topologies are very promising in small power applications.*

**Key words:** Resonant DC/DC Converter, Frequency Control, Resonant Rectifier, Transformer Magnetics, Half Bridge Topology

## 1 Introduction

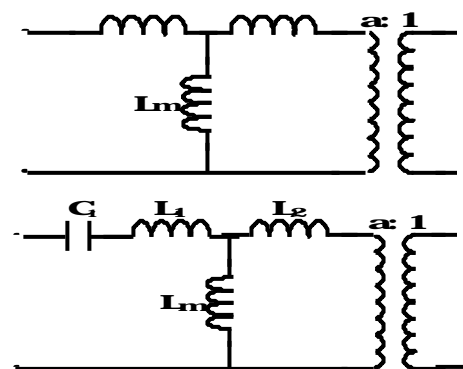
In Power converter applications where input-output ohmic isolation is mandatory or preferred, a transformer is used and to reduce the overall size of the converter, the switching frequency is stepped up. For hard-switched converters increase in operating frequency results in increased switching losses, whereas owing to the advantages of Zero Voltage Switching (ZVS) and/or Zero Current Switching (ZCS), the resonant converter may be designed to operate at very high frequency [1-21].

Depending on the topological configurations, resonant converters exhibit a wide range of characteristics. For the voltage fed network, the basic two-element topologies have their pros and cons and to improve upon the same, multi-element structures are investigated [3-9]. Also, after Steigerwald [3] explained the advantages (i.e. ZVS turn-on and almost loss free turn-off) to operate a resonant converter in the lagging power factor mode, operation in this mode has become a standard practice. Although multi-element topology offers excellent characteristics but increases size and cost. Interestingly transformer coupled converters may be configured around the transformer by properly taking into account the transformer parameters [10-13]. In this context, this

paper shows a new direction as to how the transformer parameters may be best utilized and presents the performance and control of novel DC/DC and AC/DC converter topologies.

## 2 Development of the Proposed System

The simplified transformer equivalent circuit (ignoring the core loss) is shown in Fig.1. Usually for a normal transformer the leakage (primary and secondary) inductances are too small and the magnetizing inductance is too large and hence are not suitable to replace any of the inductances used to form the resonant topology. In earlier publications authors presented a CLL topology which is ideal to operate in the lagging power factor mode and offer excellent characteristics [21]. However, the network requires two inductors and therefore bigger in size. Interestingly if a capacitor is only added to the transformer equivalent circuit a  $CL^3$  type of topology results and if the primary leakage can be made negligible then the topology becomes the CLL. This paper shows that the  $CL^3$  topology is also equally suitable to operate in the lagging power factor mode and proposes a simple realization of the network for both DC/DC and AC/DC applications.



Top: Simplified Equivalent Circuit of the Transformer.  
Bottom: The  $CL^3$  Topology Realized by a Specially Designed Transformer with only a Capacitor.

**Fig.1. Development of the Proposed Topology.**

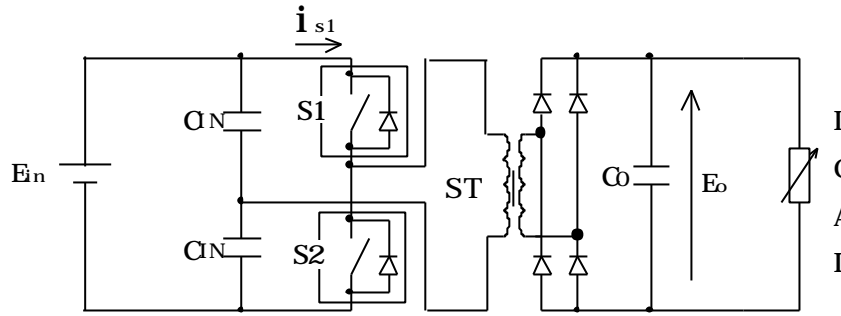


Fig.2a. Proposed DC/DC Converter.

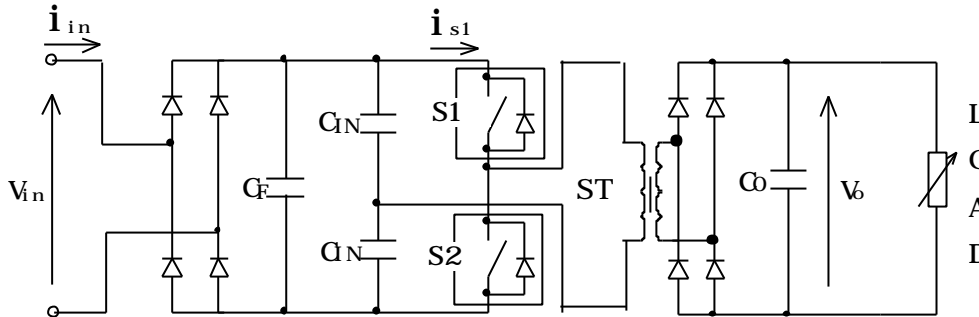


Fig.2b. Proposed AC/DC Converter.

Fig.2. shows the DC/DC and AC/DC Resonant converter topologies which use a specially designed transformer (ST). The special transformer offers three adjustable inductances. The voltage splitting capacitors are used as the capacitor ( $C_1=2C_{IN}$ ) in the resonant network. Half bridge inverter is used to reduce the device count. In the case of AC/DC converter an additional capacitor  $C_f$  is used to filter out the high frequency current components generated due to the inverter switching.

The special transformer with higher leakage and lower magnetizing inductance may be realized in a number of ways. A simpler one utilizing E-I type ferrite core is shown in Fig.3. Windings are placed on the outer limbs. Inductances are adjusted by controlling the three airgap lengths ( $l_{g1}$ ,  $l_{g2}$  and  $l_{g3}$ ).

Where,

$$x=(w/w_0), \quad g=g_1=g_2, \quad Q=w_0(1+g)L_m/R$$

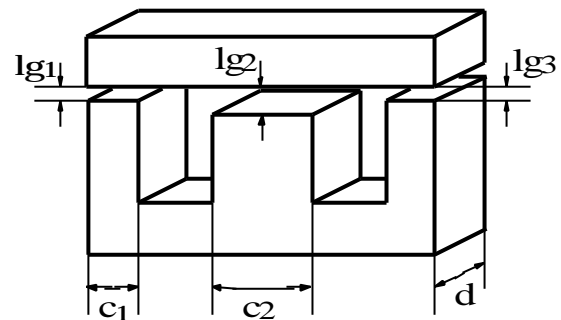


Fig.3. Transformer Core Details.

### 3 Converter Performance

Due to specific advantages [3] the converter is operated only in the lagging power factor mode and at rated load the current phase lag is reduced to minimum to consume minimum VA to supply the rated load power (watts). AC sinusoidal analysis has been carried out to bring out the important features of the network. Also converter components and devices are considered to be ideal. The simplified equivalent circuit is shown in Fig.4. The expression for the converter AC gain may be expressed as,

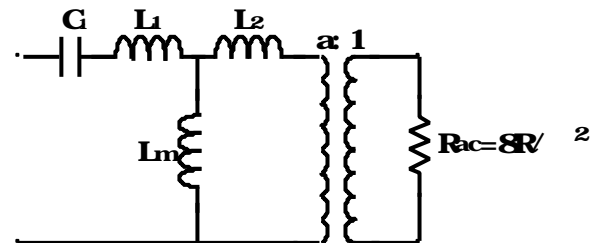


Fig.4. Simplified Equivalent Circuit ( $R=$  Load Resistance).

$$M = \frac{1}{a \sqrt{\left\{ \left( 1+g \left( 1 - \frac{1}{x^2} \right) \right)^2 + \frac{p^4 Q^2}{64a^4} \left\{ \frac{(2g+g^2)x}{(1+g)} - \frac{(1+g)}{x} \right\}^2 \right\}}}$$

Fig.5 shows the converter gain ( $M$ ) vs. frequency ratio ( $=\omega/\omega_0$ ) characteristic for  $\gamma_1 (=L_1/L_m)=1.0$  and  $\gamma_2 (L_2/L_m)=1.0$  and for different magnitudes of  $Q (=0, 1$  and  $10)$ . It has been observed that at the point "A" (determined by the frequency ratio and  $\gamma$ 's), the

converter exhibits load-independent feature. Interestingly if a converter is designed to operate at the point “A” at rated load, then with the decrease in load current, the converter automatically enters in the lagging power factor mode. Thus in the full operation range the converter operates in the lagging power factor mode, dispensing with the need of device snubber [3]. To compensate for the variation in input voltage, the converter need to be designed corresponding to the minimum input voltage and maximum load current and for all other loading conditions, the frequency may be controlled to keep output voltage constant. Fig.6 shows the effect of secondary leakage (in terms of  $\gamma_2$ ). It is clear that only a specific amount of leakage provides best operation. In Fig.6, the curve corresponding to  $\gamma_2=0$  displays the characteristic of a PRC. Thus the improvement of the topology over the usual PRC is appreciated. The boosting of voltage with load enables this converter to operate with minimum frequency variation. This explains the requirement of proper attention to all the existing inductances in the inductor-transformer to obtain optimum performance. Different other transformer core configurations are under investigations.

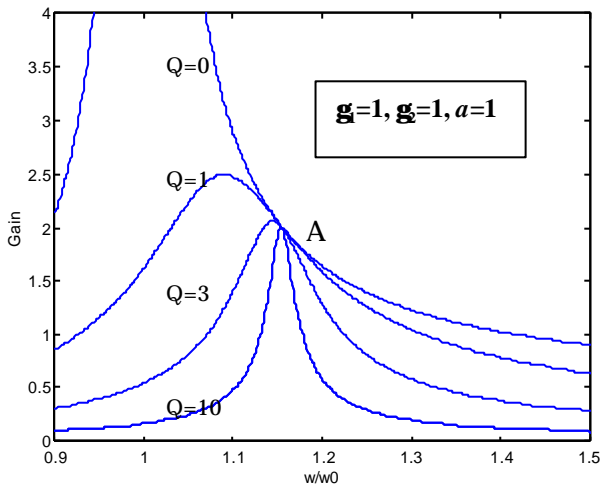


Fig.5.  $M$  vs.  $w/w_0$  characteristic for different  $Q$ .

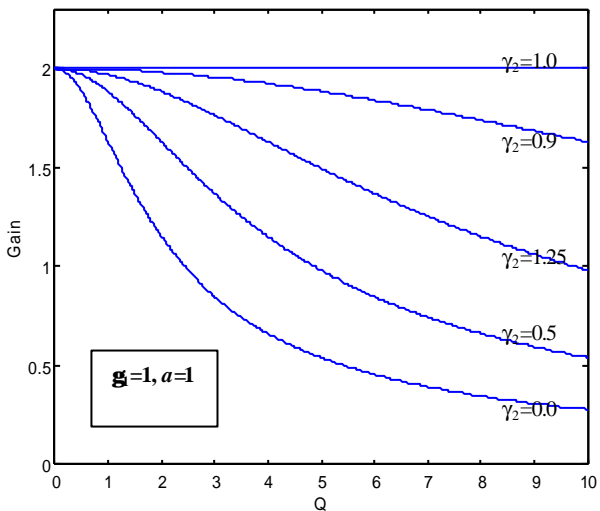


Fig.6.  $M$  vs.  $w/w_0$  characteristic for different  $g$ .

For the purpose of design, a new design variable  $\beta$ , which is the ratio of currents flowing through the transformer primary in the case of no-load and full load conditions respectively has been defined. Thus knowing  $\beta$  and  $M$ , the converter components may be found from the following equations,

$$L_m = \left(\frac{8}{p^2}\right) a^2 \frac{R}{wb} \quad C_1 = 2C_m = \frac{aM}{(a^2 M^2 - 1)w^2 L_m}$$

$$L_1 = L_2 = \left(\frac{8}{p^2}\right) a^2 \frac{(aM-1)R}{wb}$$

It is to be noted that the inductance magnitudes are inversely proportional to  $\beta$ . Therefore a higher  $\beta$  offers smaller size but at the cost of low part load efficiency. This calls for a compromise between converter performance and size reduction. A higher  $\beta$  also allows the converter to have increased output voltage and also more “selectivity”.

Finally, the gap lengths are to be determined. For simplification, the reluctance of the core is neglected compared to that of the air gap and the fringing flux around the edges, is taken into consideration by assuming that the region of uniform flux density extends outward from each of the gap edge by a length equal to half of the gap length [10,11]. After algebraic simplification, ignoring the higher order terms, the following closed form equations may be found,

$$l_{g1} = l_{g3} = \frac{c_1 d m_0 N_1^2}{(aM + 1)L_m - (c_1 + d)m_0 N_1^2}$$

$$l_{g2} = \frac{c_2 d m_0 N_1^2}{(a^2 M^2 - 1)L_m - (c_2 + d)m_0 N_1^2}$$

For AC/DC applications, the converter may be thought of as a diode rectifier fed DC/DC converter. The input AC voltage is rectified and the unfiltered DC voltage is applied to the DC/DC converter. As the switching frequency of the inverter is quite high compared to that of the power frequency, the voltage applied to the inverter appears to be almost DC and thus the converter components may be designed corresponding to the maximum power transfer condition [14,17].

## 4 Converter Control

### 4.1 For DC/DC Converter

A PI controller fed VCO (Voltage Controlled Oscillator) type control scheme is found suitable for such type of converter. The controller senses the output voltage, compares the same with a reference generating an error, which is processed by the PI controller. The PI controller output is fed to the VCO to generate the necessary gate drive signals of the IGBTs. Details of the control blocks are shown in Fig.7. It is to be noted that when operated at or near the point “A”, the network requires short circuit protection. As the voltage across the capacitor increases monotonically with the increase of the load, the capacitor voltage is sensed, compared with a

reference and if exceeded, the gate drive of the IGBT is withdrawn. This has the advantage of requiring no current sensor for safe operation of the system.

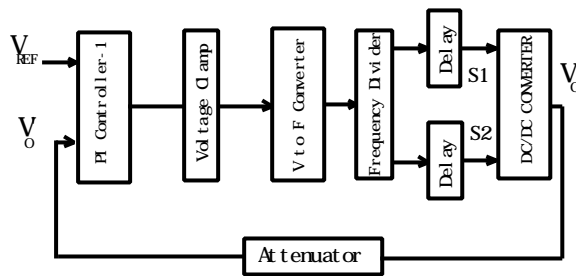


Fig.7. Control Schematics for DC/DC Converter

#### 4.2 For AC/DC Converter

The controller in AC/DC converter has to serve the dual purpose of output voltage control and input current shaping. The output voltage control method is carried out in the same as of the DC/DC converter. However, depending on the technique of the input current shaping, two new control strategies have been developed as shown in Figs.8 and 9.

To develop the control schemes the converter is initially operated only with the voltage control hardware and the converter input current is observed. A sample nature of the converter input current is shown in Fig.10. The desired waveform being a sinewave (shown with broken lines in the figure), the waveform from experiment shows that the converter draws less current near the zero crossing and more current near the voltage peak. As the converter is operated always in the lagging power factor mode a monotonous gain-frequency relation exist, which may be exploited to improve upon the converter input current waveform. The technique is through fixed frequency modulation by reducing frequency near the zero crossing and increasing the same near the peak. Reduction in frequency reduced the equivalent impedance and thus draws more current and vice versa. This control scheme is simple requiring no current sensor.

To further improve the converter input current use of a current sensor is recommended. The input current is sensed and compared with a reference generating an error which is processed by a PI controller, the output of which drives the VCO. The details of the scheme is shown in Fig.9. Two PI controllers are used as shown.

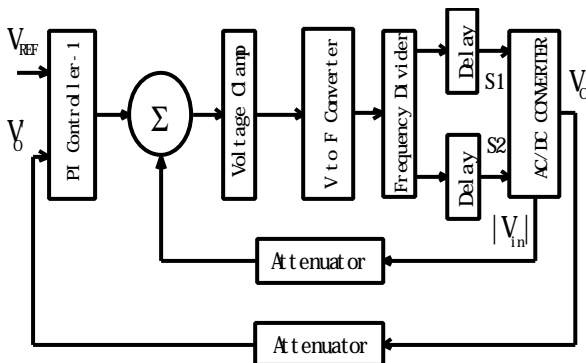


Fig.8. Control Scheme-1.

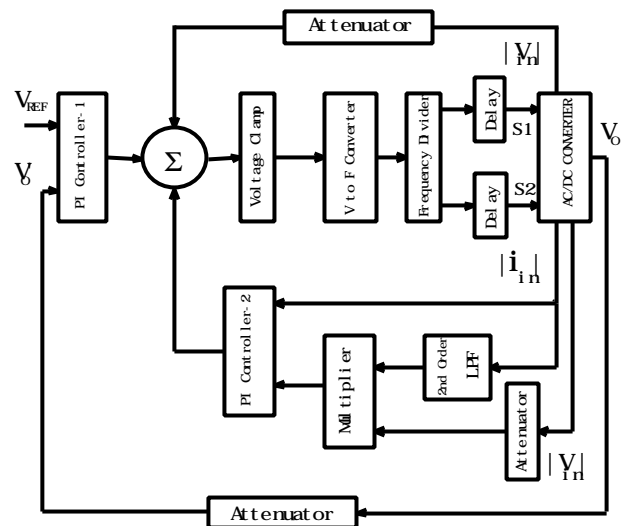


Fig.9. Control Scheme-2.

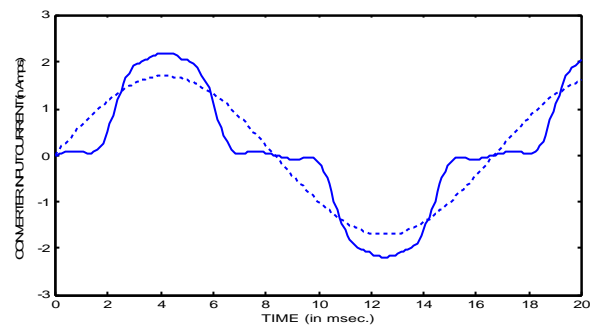


Fig.10. Converter Input Current Waveform With No Current Control.

### 5 Experimental Results

#### 5.1 For DC/DC Converter

An experimental prototype of the converter has been fabricated in the laboratory. A 48V input and 24V, 1A output DC/DC converter application has been considered. A transformer with “1:1” turns ratio is produced with  $L_1=65.8\mu\text{H}$ ,  $L_2=64.6\mu\text{H}$  and  $L_m=54\mu\text{H}$ . The corresponding gap lengths are  $l_{g1}=l_{g2}=0.25\text{mm}$ ,  $l_{g3}=0.4\text{mm}$ . A capacitor  $C_{IN}=0.11\mu\text{F}$  has been used. Operating frequency is considered to be around 35 kHz. The controller is also realized and found to perform satisfactorily. Fig.11 shows the waveform for full load and half load conditions. Only a frequency increment of 1.01kHz is required, which is automatically adjusted by the controller. The converter is decided to operate well in the lagging power factor mode, so that, in case of overload and/or input voltage fluctuations, it remains still in the same mode. The converter operates just in the lagging power factor mode in the case of minimum input voltage and maximum output current. As the peak voltage across capacitor  $C_{IN}$  increases monotonically with the load current, therefore this voltage is sensed and compared with a maximum allowable reference, which when exceeded the gate drive of the devices are withdrawn to protect the devices.

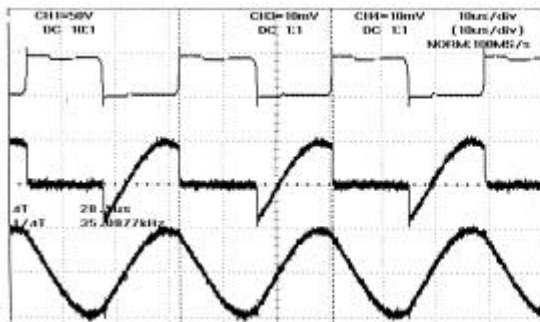
## 5.2 For AC/DC Converter

For AC/DC application an arbitrary rating of 75V(rms) input and 25V, 4A DC output is considered. A filter capacitor  $C_F$  of  $1\mu\text{F}$  is used. It is to be noted that a larger  $C_F$  may distort the rectified voltage substantially, which is undesirable, whereas a smaller  $C_F$  may not sufficiently filter out high frequency current components generated by the inverter switching. The resonant network is realized by the special transformer (ST) and capacitors  $C_{IN}$  ( $=0.11\mu\text{F}$ ). All three types of controllers discussed earlier have been fabricated and experimented. For the case with no current control a peaky current waveform is noted as shown in Fig.12. The Total Harmonic Distortion (THD) is found to be 20.8%.

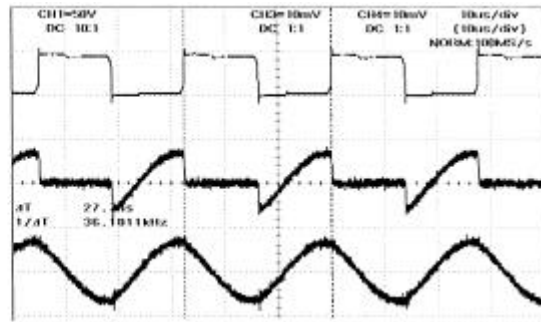
To improve the converter input current waveform, the

Control Scheme-1 is implemented. A small voltage proportional to the rectified input voltage is added to the output of the PI Controller to have fixed frequency modulation. Fig.13 shows the corresponding waveforms. The THD is found to be 9.4%. Considering that no current sensor and associated circuitry is used, the scheme seems very attractive. The operating frequency is found to vary in the range of 34.48kHz to 41.84kHz.

To further improve the current waveform, a current sensor is used. The input current is sensed and compared with a sinusoidal current reference generating an error, which is processed by the PI Controller-2. Fig.14 shows the related waveforms. A THD of 4.1% has been noted. Considering that the normal supply voltage usually has a THD of 2%. The performance of Scheme-2 is excellent but at the cost of increased complexity and cost.



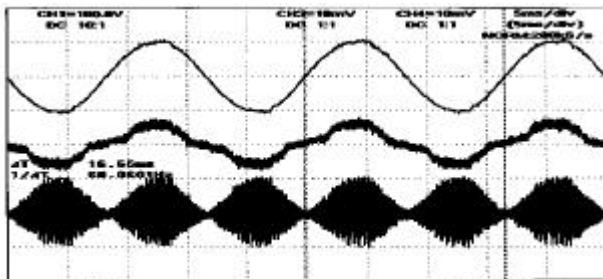
(Top:  $V_{s1}$  Middle:  $i_{s1}$  Bottom:  $i_{ST}$ )  
For Full Load Condition



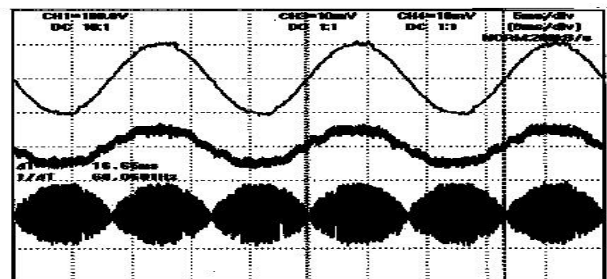
(Top:  $V_{s1}$  Middle:  $i_{s1}$  Bottom:  $i_{ST}$ )  
For Half Load Condition

Volt Scale: 50V/div. Amp Scale: 5A/div. Time Scale: 10μs/div.

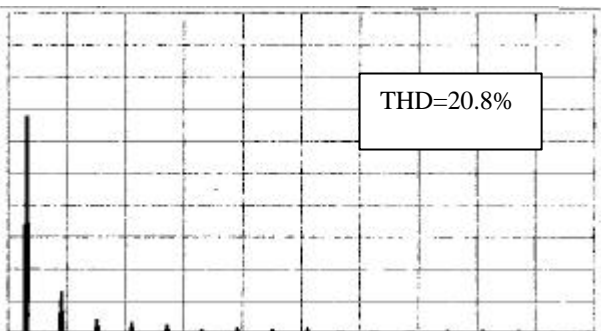
**Fig.11. Experimental Waveforms For DC/DC Converter.**



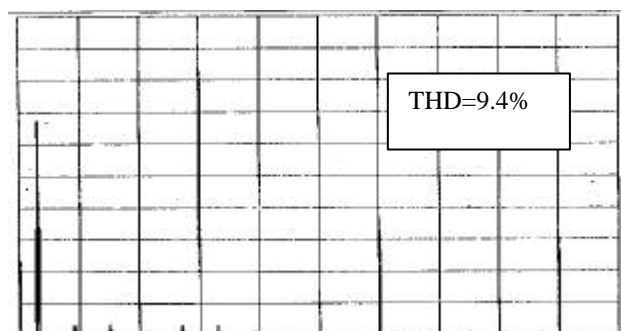
(Top:  $V_{in}$  Middle:  $i_{in}$  Bottom:  $i_{s1}$ )  
Scale: Top=100V/div. Middle=2A/div. Bottom=10A/div.  
Fig.12a. Voltage and Current Waveforms.



(Top:  $V_{in}$  Middle:  $i_{in}$  Bottom:  $i_{s1}$ )  
Scale: Top=100V/div. Middle=2A/div. Bottom=10A/div.  
Fig.13a. Voltage and Current Waveforms.



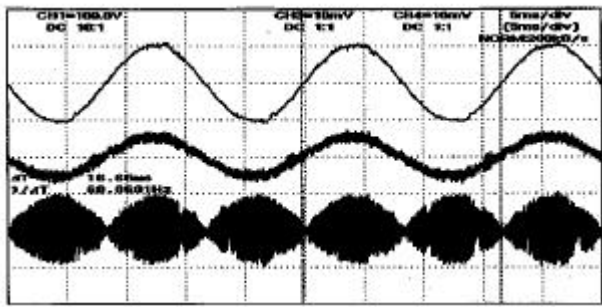
(Horizontal Full Range=0-2kHz Vertical Full Range=0-1V)  
Fig.12b. Harmonic Spectrum of Converter Input Current.



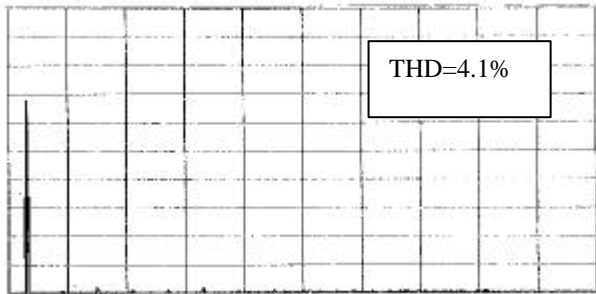
(Horizontal Full Range=0-2kHz Vertical Full Range=0-1V)  
Fig.13b. Harmonic Spectrum of Converter Input Current.

**Fig.12. Experimental Waveforms With No Current Control.**

**Fig.13. Experimental Waveforms With Control Scheme-1 in Operation.**



(Top:  $V_{in}$  Middle:  $i_{in}$  Bottom:  $i_{s1}$ )  
Scale: Top=100V/div. Middle=2A/div. Bottom=10A/div.  
Fig.14a. Voltage and Current Waveforms.



(Horizontal Full Range=0-2kHz Vertical Full Range=0-1V)  
Fig.12b. Harmonic Spectrum of Converter Input Current.

**Fig.14. Experimental Waveforms  
With Control Scheme-2 in Operation.**

## 6 Conclusions

This paper introduces a new way to realize transformer coupled resonant converters by properly utilizing the transformer parameters. For such purpose the transformer is specially designed with increased leakage and reduced magnetizing inductances. Adding only a capacitor a series parallel  $CL^3$  topology is formed which is very suitable to operate in the lagging power factor mode dispensing with the need for a device snubber. Also proper design of such converters will enable the same to operate with minimum variation in operating frequency despite change in operating conditions. Several aspects for DC/DC and AC/DC converters have been discussed. Novel control methods have been reported in the case of AC/DC converters, which will keep output voltage constant and also shape the converter input current as well. Laboratory prototypes of both DC/DC and AC/DC converters have been realized and excellent performances have been confirmed. The proposed control method for AC/DC converter yields a THD as low as 4.1% for the converter input current while smoothly controlling the converter output voltage. These types of converters are very promising particularly in the small output range.

## References

- [1] V.T.Ranganathan, P.D.Ziogas and V.R.Stefanovic, "A regulated dc-dc voltage source converter using a high frequency link," IEEE Trans. on Ind. Appl., Vol.18, pp.279-287, No.3, 1982.
- [2] R.Oruganti and F.C.Lee, "Resonant power processors, Part I-State plane analysis," IEEE Trans Ind. on Appl. Vol.21, pp.1453-1960, 1985.
- [3] R.L.Steigerwald, "A comparison of half-bridge resonant

- converter topologies," IEEE Trans. on Pwr. Ecs., Vol.3, pp.174-182, 1988.
- [4] A.K.S.Bhat and M.M.Swami, "Analysis of parallel resonant converter operating above resonance," IEEE Trans. on Aero. & Elec. Sys., Vol.25, pp.449-458, 1989.
- [5] T.Ninomiya, M.Nakahara, T.Higashi and K.Harada, "A unified analysis of resonant converters," IEEE Trans. on Pwr. Ecs. Vol.6, No.2, pp.260-270, 1991.
- [6] R.P.Severns, "Topologies of three-element converters," IEEE Trans. on Pwr. Ecs., Vol.7, pp.89-98, 1992.
- [7] I.Batarseh, "Resonant converter topologies with three and four energy storage elements", IEEE Trans. on Pwr. Ecs., Vol.9, pp.64-73, 1994.
- [8] S.Hamada and M.Nakaoka, "Analysis and design of saturable reactor assisted soft-switching DC-DC converter," IEEE Trans. on Pwr. Ecs. Vol.9, No.3, pp.309-317, 1994.
- [9] J.H.Cheng and A.F.Witulski, "Analytic solution for LLC parallel resonant converter simplify use of two- and three-element converters", IEEE Trans. on Pwr. Ecs. Vol. PE-13, pp.235-243, 1998.
- [10] S.B.Dewan, J.D.Lavers and H.A.Kojori, "The effect of the circuit leakage inductances on the steady state performance of an inductor-transformer resonant dc-dc converter," IEEE Trans. on Mag., Vol.23, No.5, pp.2785-2787, 1987.
- [11] H.A.Kojori, J.D.Lavers and S.B.Dewan, "State plane analysis of a resonant dc-dc converter incorporating integrated magnetics," IEEE Trans. on Mag., Vol.24, No.6, pp.2898-2900, 1988.
- [12] R.Farrington, M.M.Jovanovic and F.C.Lee, "A new family of isolated converters that uses the magnetizing inductance of the transformer to achieve zero-voltage switching," IEEE Trans. on Pwr. Ecs., Vol.8, No.4, pp.535-545, 1993.
- [13] H.J.Jiang, G.Maggetto and P.Lataire, "Steady-state analysis of the series resonant DC-DC converter in conjunction with loosely coupled transformer-above resonance operation," IEEE Trans. on Pwr. Ecs., Vol.14, No.3, pp.469-480, 1999.
- [14] M.J.Schutten, R.L.Steigerwald and M.H.Kheraluwala, "Characteristics of Load Resonant Converters Operated in a High-Power Factor Mode," IEEE Trans. on Pwr. Ecs., Vol.7, No.2, pp.304-314, 1992.
- [15] W.Sulistiyono and P.Enjeti, "A Series Resonant AC-to-DC Rectifier With High-Frequency Isolation," IEEE Trans. on Pwr. Ecs., Vol.10, No.6, 1995.
- [16] J.Hong, D.Maksimovic, R.W.Ericson and I.Khan, "Half Cycle Control of the Parallel Resonant Converter Operated as a High Power Factor Rectifier", IEEE Trans. on Pwr. Ecs., Vol.10, No.1, pp.1-8, 1995.
- [17] V.Belaguli and A.K.S.Bhat, "Operation of the LCC Type Parallel Resonant Converter as a Low Harmonic Rectifier", IEEE Trans. on Ind. Ecs., Vol.46, No.2, pp.288-299, 1999.
- [18] H.Pinheiro, P.Jain and G.Joos, "Series-Parallel Resonant Converter in the Self-Sustained Oscillating Mode for Unity Power Factor Applications", APEC'97, pp.477-483.
- [19] V.R.Durgesh, A.Muthuramalingam and V.V.Sastry, "Operation of Fixed Frequency Class-D Series-Parallel Resonant Converter on Utility Line With Active Control", APEC'99, pp.375-381.
- [20] S.V.Mollov and A.J.Forsyth, "Analysis, Design and Resonant Current Control for a 1-MHz High-Power-Factor Rectifier," IEEE Trans. on Ind. Ecs., Vol.46, pp.620-627, 1999.
- [21] C.Chakraborty and M.Ishida, "Improved Performance Resonant Rectifier: Prospective Topology and Control Schemes," Accepted in IEEE IAS-2000 Conf., Oct. 8-12, 2000, Rome, Italy.